Journal of Inorganic Biochemistry 123 (2013) 11–17

Contents lists available at SciVerse ScienceDirect

Journal of Inorganic Biochemistry

journal homepage: www.elsevier.com/locate/jinorgbio

Luminescent material based on the $[Eu(TTA)_3(H_2O)_2]$ complex incorporated into modified silica particles for biological applications

Ana Valéria S. Lourenço [a], Cláudia A. Kodaira [b,1], Eduardo M. Ramos-Sanchez [c,2], Maria Cláudia F.C. Felinto [d,3], Hiro Goto [e,4], Magnus Gidlund [c,2], Oscar L. Malta [f,5], Hermi F. Brito [a,*]

[a] Instituto de Química, Universidade de São Paulo, CP 26077, 05508-000 São Paulo, Brazil
[b] Luminetech Marcadores Ópticos Ltda — CIETEC, Av. Prof. Lineu Prestes, 2242 Sala 9 2ª andar, 05508-000 São Paulo, SP, Brazil
[c] Departamento de Imunologia, Instituto de Ciências Biomédicas-IV, Universidade de São Paulo, Av. Lineu Prestes, 1730, 05508-900 São Paulo, Brazil
[d] Instituto de Pesquisas Energéticas e Nucleares, Av. Lineu Prestes, 2242, 05508-000 São Paulo, Brazil
[e] Faculdade de Medicina e Instituto de Medicina Tropical de São Paulo, Universidade de São Paulo, Av. Dr. Enéas de Carvalho Aguiar, 470, 05403-000 São Paulo, Brazil
[f] Departamento de Química Fundamental, CCEN, Universidade Federal de Pernambuco Cidade Universitária, 50670-901 Recife, Brazil

ARTICLE INFO

Article history:
Received 17 October 2012
Received in revised form 16 February 2013
Accepted 18 February 2013
Available online 26 February 2013

Keywords:
Europium complex
Functionalized silica
Luminescence properties
Bioassay
Oxidized low density lipoprotein

ABSTRACT

Amino-functionalized luminescent silica particles were investigated for use in immunoassays. The particles were prepared by the *Stöber method* where the $[Eu(TTA)_3(H_2O)_2]$ complex (TTA: 3-thenoyltrifluoroacetonate) was incorporated into silica particles during the hydrolysis and condensation of TEOS: tetraethylorthosilicate. Then, the amino groups were introduced in the particle surface using APTS: 3-aminopropyltriethoxisilane. The resulting particles were characterized by scanning electron microscopy (SEM), X ray diffraction (XRD) and photoluminescence spectroscopy. In order to demonstrate the viability of the use of luminescent particles as optical markers, an enzyme–substrate reaction was performed using HRP: horseradish peroxidase. It was possible to verify the binding of HRP-oxidized LDL (low density lipoprotein) and anti-oxLDL antibody-luminescent silica particles through the evaluation of the presence of HRP. The bioassay data open a broad field for the development of protein-tagged luminescent particles for use in biomedical sciences.

1. Introduction

Nowadays the development of luminescent complexes incorporating silica, which combine the characteristics of inorganic matrices and optical properties of the rare earth complexes, has been the subject of several studies [1–4]. There has been an increasing interest in this field of research, where silica particles were shown to be very useful platforms for lighting and luminescent markers or probes [5–9]. The trivalent rare earths (RE^{3+}) show unique properties [10] and have been widely applied in biological assays [11]. The criteria that should accomplish a RE^{3+} luminescent probe to be helpful in the design of bioassays in diagnostic or drug discovery (high throughput screening) are defined as brightness, absorption wavelength, luminescence decay, instrumentation crosstalk, stability, lipophilicity/hydrophilicity, photobleaching, quenching phenomenon, conjugation chemistry, and synthesis practicability.

The 4f orbitals are shielded from the chemical environment by the 5s and 5p filled orbitals, producing very narrow bands in their emission and absorption spectra from the compounds and long lifetimes [10,12]. Furthermore, the surface of the silica particles incorporating RE^{3+}-complexes can be easily modified, providing new opportunities for their applications in biological assays, enabling conjugation with biomolecules such as proteins, peptides, sugars, antibodies, etc. [13–15].

Ischemic coronary artery disease consequent of atherosclerotic process may lead to an inadequate blood circulation in the myocardium due to partial or complete obstruction of the coronary arteries [16]. Atherosclerosis is responsible for more than 30% of the total number of recorded deaths in the urban centers. The process is a chronic inflammatory disease characterized by the accumulation of lipid and vascular smooth muscle cell proliferation on the wall of the artery [17,18].

Clinical evidences demonstrate that high plasma concentration of low density lipoprotein (LDL) is a risk factor for atherosclerosis development. Indeed the modified forms of LDL as oxidized LDL (oxLDL) are the main components responsible for the formation of foam cells, contributing to the installation of the atherosclerotic process [19,20].

This study presents a preparation of a luminescent marker based on silica particles incorporating $[Eu(TTA)_3(H_2O)_2]$, where TTA: 3-thenoyltrifluoroacetonate. In addition, the recognition of the conjugation between the marker incubated with anti-oxLDL antibody

* Corresponding author. Tel.: +55 11 3091 3708; fax: +55 11 3091 3146.
E-mail address: hefbrito@iq.usp.br (H.F. Brito).
[1] Tel.: +55 11 3039 8432.
[2] Tel.: +55 11 3091 7382; fax: +55 11 3091 7224.
[3] Tel.: +55 11 3133 9343; fax: +55 11 3133 9018.
[4] Tel.: +55 11 3061 7023; fax: +55 11 3061 8270.
[5] Tel.: +55 81 2126 7459; fax: +55 81 2126 8442.

0162-0134/$ – see front matter © 2013 Elsevier Inc. All rights reserved.
http://dx.doi.org/10.1016/j.jinorgbio.2013.02.006

and the oxLDL labeled with horseradish peroxidase (HRP) was investigated, using enzyme–substrate reaction.

2. Experimental

2.1. Preparation of the $[Eu(TTA)_3(H_2O)_2]$ complex incorporated with amino-functionalized silica particles

The luminescent amino-functionalized silica particles were prepared using the modified Stöber method [21]. Complex diaquatris (thenoyltrifluoroacetonate) europium(III) (1.9 mmol), named as Eu-TTA, prepared by the method reported elsewhere [22,23] was dissolved in 100 mL of ethyl alcohol (Aldrich). Afterwards, 1.4 mmol of TEOS: tetraethylorthosilicate (Fluka) and 2 mL of hydrous ammonia 28% (Synth) were added to the previous solution at room temperature for 12 h under stirring. Then, the precipitate was centrifuged and washed with water and ethyl alcohol. Subsequently, the resulting particles were redispersed in ethyl alcohol (100 mL) and functionalized with 0.2 mmol of APTES: 3-aminopropyltriethoxisilane (Fluka) and stirred at room temperature for 5 h [24]. Finally, the luminescent amino-functionalized silica particles (named as Eu-TTA-Si) were centrifuged, washed with water and ethyl alcohol and dried at 100 °C overnight.

X ray powder diffraction patterns were recorded on a Rigaku Miniflex using Cu Kα radiation (30 kV and 15 mA) in the range from 5 to 70° (2θ). The scanning electron microscopy (SEM) micrographs were obtained in a Field Emission Scanning Electron Microscope model JEOL JSM 7401F. The solid samples were deposited on a double-sided copper tape, attached to the sample holder. The excitation and emission spectra of the complex and amino-functionalized material at liquid nitrogen temperature (77 K) were recorded at an angle of 22.5° (front face) in a spectrofluorimeter (SPEX-Fluorog 2) with double grating 0.22 monochromator (SPEX 1680) and a 450 W Xenon lamp as excitation source. All spectra were recorded using a detector mode correction. The luminescence decay curves of the emitting levels were measured at room temperature using a phosphorimeter SPEX 1934D accessory coupled to the spectrofluorometer.

2.2. Antigen-antibody (Ag–Ab) interaction on the surface of the luminescent amino-functionalized silica particles

2.2.1. Bioconjugation of Eu-TTA-Si particles with anti-oxLDL antibody

The process for the bioconjugation of anti-oxLDL antibody [19,25] onto the luminescent amino-functionalized silica particles is shown in Fig. 1 [11]. The Eu-TTA-Si particles (1.0 mg) were dispersed in phosphate-buffered saline (PBS) solution (pH 7.4) containing 5% glutaraldehyde — GA (Aldrich) and kept at 4 °C for 12 h. After that, these particles were centrifuged, washed four times with a PBS solution and redispersed in 1.0 mL of PBS solution. At that time, 30 μL of anti-oxLDL antibody solution (1.9 mg mL^{-1}) was added and incubated overnight at 4 °C. Then, 1.6 mg of sodium borohydride ($NaBH_4$ from Merck), was added and left to react for 30 min at 4 °C. To block the unreacted aldehyde sites, 50 μL of glycine (Vetec) solution 0.5 mol L^{-1} was added, and this mixture was maintained for 2 h at 4 °C. The conjugate system Eu-TTA-Si particle-GA-anti-oxLDL was obtained and washed four times with PBS solution to remove the excess of glycine, and afterwards stored at 4 °C.

2.2.2. Conjugation of HRP-GA with oxLDL

Different HRP amounts from Aldrich (2 to 370 units) were added in 1.0 mL of PBS buffer (pH 7.4) and 18.75 μL of glutaraldehyde solution (50%) and kept for 12 h at 4 °C. The HRP concentration (in U mL^{-1}) was found as the difference between initial and final enzyme amount remaining in the solution, at all times the specific activity was expressed in terms of pyrogallol units (one pyrogallol unit will form 1.0 mg purpurogallin from pyrogallol in 20 s with pH 6.0 at 20 °C). The solutions were dialyzed in a molecular porous membrane

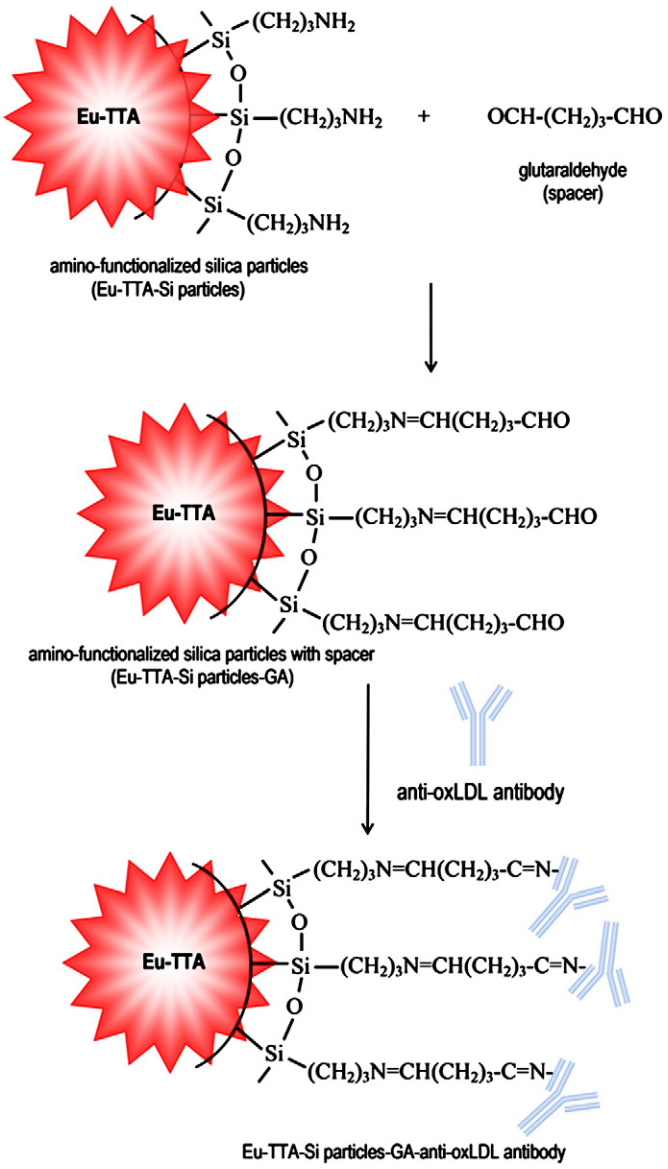

Fig. 1. Representative scheme of the immobilization of anti-oxLDL antibody particles in Eu-TTA-Si using glutaraldehyde as a spacer.

tubing (Spectrum Laboratories, 12–14,000 (molecular weight cut-off)) against PBS solution for 24 h at 4 °C. After this step, 85 μL of oxLDL solution (3.0 mg mL^{-1}), obtained as described in references [26,27], was incubated to the mixture for 12 h at 4 °C. Besides, 1.6 mg of sodium borohydride was added and after 30 min, 50 μL of glycine (0.5 mol L^{-1}) was added and left to react for 2 h at 4 °C. Then this solution was dialyzed against PBS solution for 24 h at 4 °C. The representation of the HRP-GA-oxLDL bioconjugated system is illustrated in Fig. 2.

2.2.3. HRP-GA-oxLDL with Eu-TTA-Si particle-GA-anti-oxLDL antibody reaction

The HRP-GA-oxLDL solution was added to Eu-TTA-Si particle-GA-anti-oxLDL antibody and incubated overnight at 4 °C (Fig. 3). After removal of the supernatant, the solid precipitate was washed fifteen times with PBS. Both the supernatant and washing water were reserved for further analysis to determine unbound HRP-GA-oxLDL.

2.2.4. Measurement of the HRP enzyme concentration

The optical density measurements of the supernatant and the washings were performed on flat bottomed 96-well polystyrene

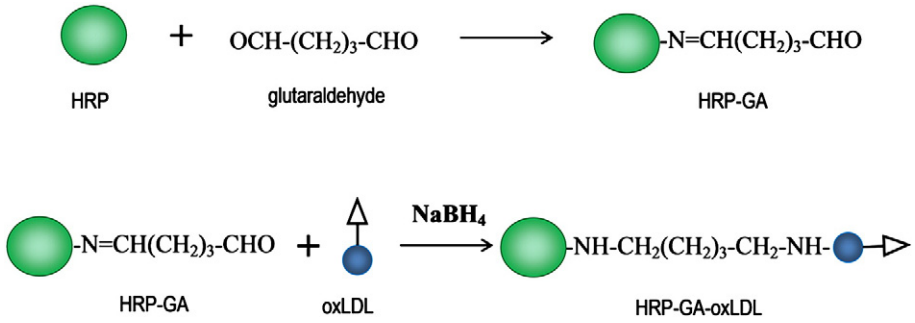

Fig. 2. Representative scheme of immobilization of the enzyme HRP with the oxLDL, using the spacer glutaraldehyde and $NaBH_4$ to stabilize the Schiff bases.

plate Corning (Costar 3590). First, the wells contain the supernatant and the washings, 100 μL of tetramethylbenzidine solution (TMB) (Sigma-Aldrich) was added to each well and the reaction was developed for 15 min at room temperature (~25 °C). Then, the reaction was stopped with 25 μL of 1.0 mol L^{-1} H_2SO_4 solution, and color development was measured at 450 nm on a Titertec Multiskan MCC/340 apparatus (Labsystems). The calibration curve was based on several dilutions of the HRP solution. Analyses were done in duplicate for all samples.

3. Results and discussion

Fig. 4 shows the XRD patterns of the Eu-TTA precursor complex and Eu-TTA-Si particles. For the Eu-TTA complex (Fig. 4a) several diffraction peaks were observed, indicating high crystallinity of the coordination compound. Moreover, the XRD patterns of the Eu-TTA-Si system (Fig. 4b) exhibit a broad band centered at $2\theta = 25°$, characteristic of amorphous silica phase, corroborating with data from the literature [2,27–30], and few diffraction peaks corresponding to the

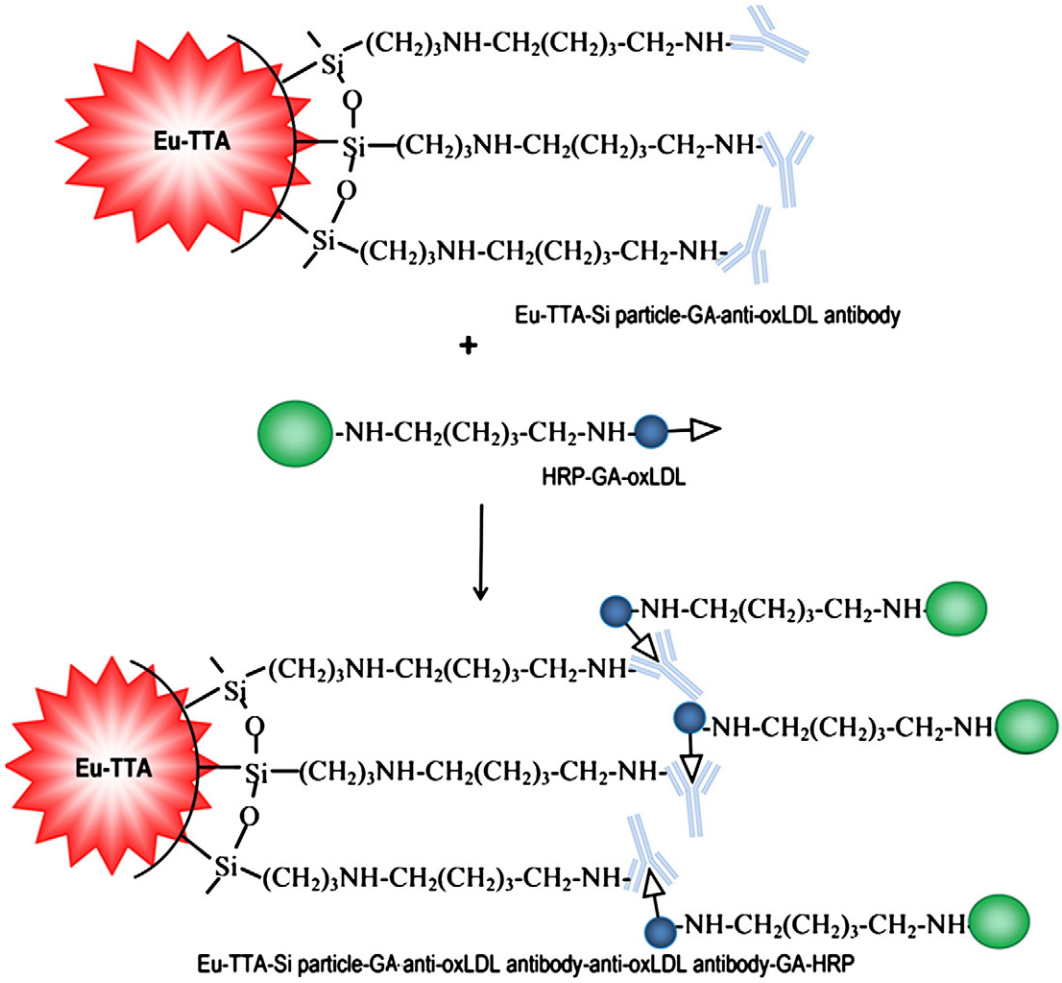

Fig. 3. Representative scheme of conjugation of the anti-oxLDL antibody with oxLDL, using the systems HRP-GA-oxLDL and Eu-TTA-Si particles-GA-anti-oxLDL.

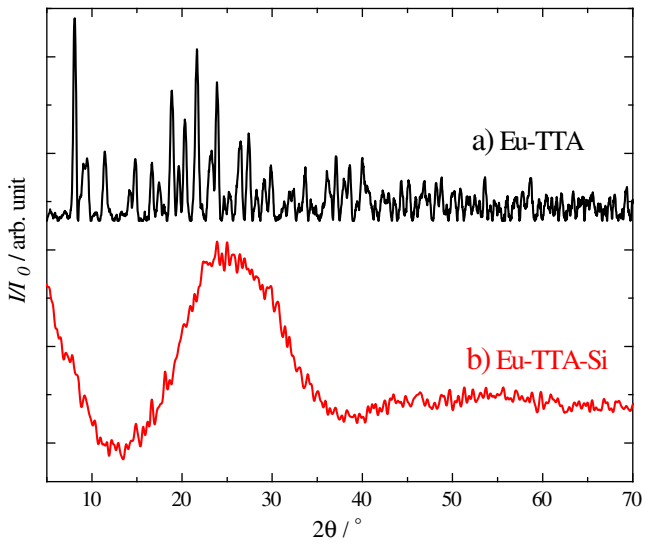

Fig. 4. X ray diffraction patterns of a) Eu-TTA complex and b) Eu-TTA-Si material.

Eu-TTA complex precursor. This indicates different interactions between the rare earth complex and the silica network in the process of silanization for the system prepared by the Stöber method [31–33].

SEM was used to observe the differences in the morphology of the Eu-TTA and Eu-TTA-Si (Fig. 5). The SEM image of Eu-TTA-Si (Fig. 5b) reveals a homogeneous material with a rough and porous surface, suggesting a silica coating in the Eu-TTA precursor complex (Fig. 5a).

The concentration of 10,899 nmol mg^{-1} of amino groups on the Eu-TTA-Si particle surface was quantified using the ninhydrin method [34,35]. Then, the potential for biological application of these particles was demonstrated with the quantification of the amine groups after the conjugation with glutaraldehyde spacer [11]. The concentration of amine groups decreases to 54.53%, suggesting that these groups react with the glutaraldehyde.

3.1. Luminescence marker study

Fig. 6 shows the excitation spectra of the Eu-TTA complex and the Eu-TTA-Si material recorded at liquid nitrogen (77 K) in the range of 250–600 nm, monitored at the $^5D_0 \rightarrow {}^7F_2$ hypersensitive transition (613 nm). The excitation spectrum of the Eu-TTA complex, Fig. 6a, displays a broad absorption band covering the spectral range from 250 to 475 nm overlapped with narrow bands assigned to the $^7F_0 \rightarrow {}^5L_6$ (394 nm), $^5D_2 \rightarrow {}^7F_0$ (464 nm) transitions of the trivalent europium ion. In Fig. 6b, the spectrum of Eu-TTA-Si shows a broad absorption

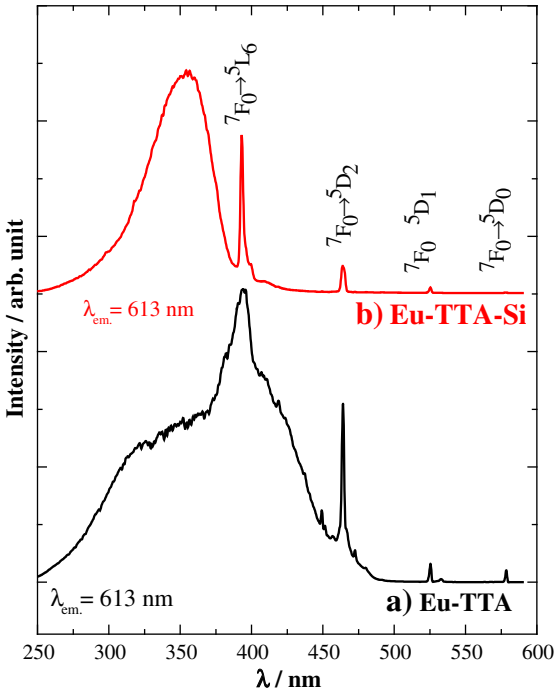

Fig. 6. Excitation spectra obtained at 77 K of a) Eu-TTA complex and b) Eu-TTA-Si material.

band, in the range 300–425 nm, which is attributed to $S_0 \rightarrow S_1$ allowed transition in the TTA ligands. The excitation spectrum also displays three narrow bands attributed to intraconfigurational transitions of the Eu^{3+} ion (Fig. 6b), assigned to $^7F_0 \rightarrow {}^5L_6$ (394 nm), $^7F_0 \rightarrow {}^5D_2$ (464 nm) and $^7F_0 \rightarrow {}^5D_1$ (525 nm). The Eu-TTA-Si material exhibits a different spectral profile compared with the Eu-TTA complex, suggesting that there was an effective interaction between the Eu-TTA complex and the silica network.

The emission spectra (Fig. 7) were also recorded at 77 K in the range of 420–750 nm, under excitation in the $^7F_0 \rightarrow {}^5L_6$ transition. The spectra exhibit narrow bands attributed to $^5D_0 \rightarrow {}^7F_J$ transitions (where J = 0, 1, 2, 3 and 4), dominated by the $^5D_0 \rightarrow {}^7F_2$ hypersensitive transition. However, the intensity of the $^5D_0 \rightarrow {}^7F_2$ transition in relation to the $^5D_0 \rightarrow {}^7F_1$ transition decreases in the emission spectra for the Eu-TTA-Si material compared with the Eu-TTA complex, suggesting that the rare earth ion is in a site with higher symmetry when coated by the silica network.

It is important to notice the absence of a broad band between 450 and 600 nm, referring to the triplet state (T) of the TTA ligand, demonstrating an efficient ligand-to-metal energy transfer. It is also observed

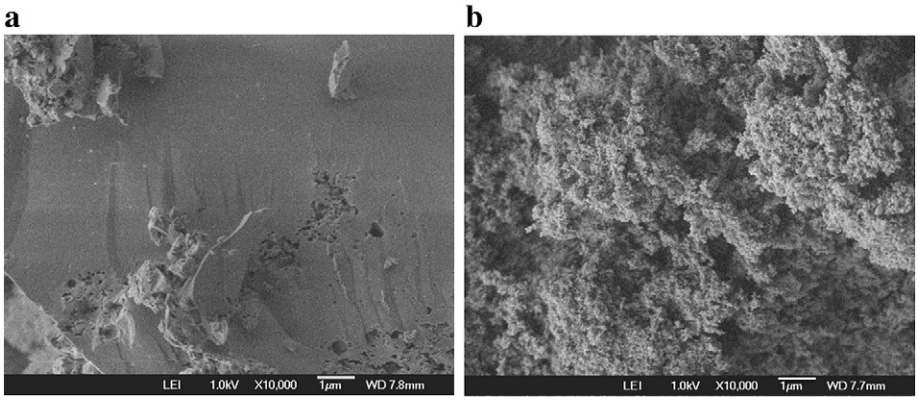

Fig. 5. The scanning electron micrographs of a) Eu-TTA complex and b) Eu-TTA-Si material.

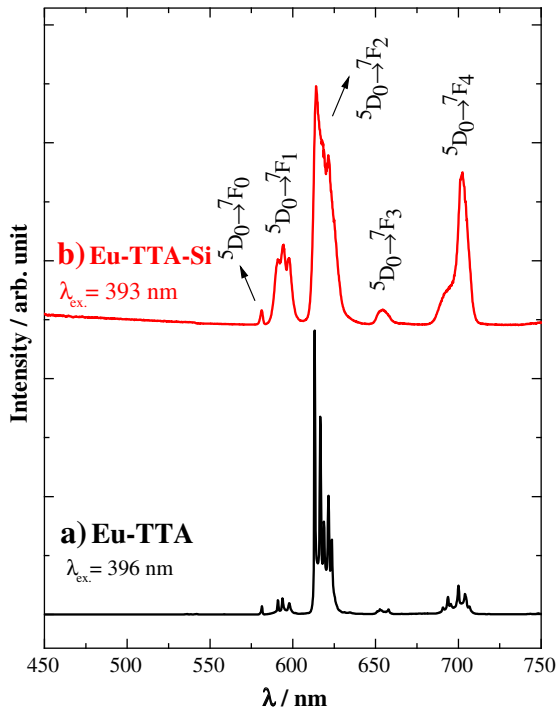

Fig. 7. Emission spectra of a) Eu-TTA complex and b) Eu-TTA-Si material, obtained at 77 K.

as a broadened peak of the $^5D_0 \rightarrow {}^7F_J$ transitions in the Eu-TTA-Si material (Fig. 7b) as compared with the complex, which can be explained by a non-homogeneity of Eu^{3+} sites due to the silica porous microstructure.

The CIE (*Comission Internacionale de l'Eclairage*) *x,y* chromaticity diagram of Eu-TTA and Eu-TTA-Si systems is displayed in Fig. 8 [36].

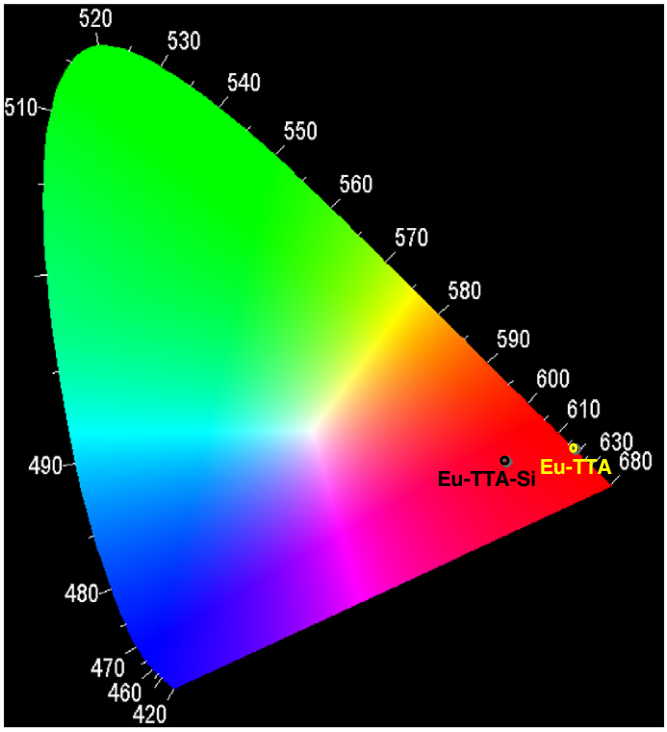

Fig. 8. CIE chromaticity diagram showing the x,y emission color coordinates for Eu-TTA and Eu-TTA-Si systems.

When the complex was incorporated in silica matrix, a gradual shift in the *x,y* color coordinates from the red to blue was observed.

The luminescence decay curves of the $^5D_0$ emitting level of the Eu-TTA complex and modified silica material were recorded under excitation at 394 nm and emission at 614 nm. These data were adjusted with a mono-exponential decay for the complex and bi-exponential for the modified silica material. The data in Table 1 show that after the silanization of the Eu-TTA complex the lifetime increases in relation to the complex precursor due to the rigidity of the silica network (Si–O) and substitution of water molecules in the first coordination sphere [37,38]. This behavior clearly indicates an interaction of the silica network with the complex, changing the environment of the Eu^{3+} ion.

The experimental intensity parameters Ω_λ ($\lambda = 2$ and 4) were determined for the Eu-TTA complex and Eu-TTA-Si material from the emission spectral data. The Ω_λ, also known as Judd–Ofelt parameters [39], are determined by the intensities of the transitions $^5D_0 \rightarrow {}^7F_J$ ($J = 2$ and 4) of Eu^{3+} ion [12,22,40], where the mechanisms of forced electric dipole and dynamic coupling are considered simultaneously. Therefore, the luminescence intensity (I) is expressed in terms of the area under the emission curves of the transitions from the $^5D_0$ level to the levels ^7F_J ($J = 2$ and 4), and is defined as:

$$I_{0\rightarrow J} = \hbar\omega_{0\rightarrow J} A_{0\rightarrow J} N_0 \quad (1)$$

where $\hbar\omega_0$ is the energy of the transition (in cm^{-1}), N_0 is the population of the emitting level $^5D_0$ and $A_{0\rightarrow J}$ is the coefficient of spontaneous emission. For the experimental determination of the emission coefficient $A_{0\rightarrow J}$ from the emission spectra the magnetic dipole used allowed $^5D_0 \rightarrow {}^7F_1$ transition, which is formally insensitive to the chemical environment around the Eu^{3+} compound and, consequently, can be used as a reference [41]. The values of Ω_λ are obtained from:

$$A_{0\rightarrow J} = \frac{4e^2\omega^3}{3\hbar c^3}\frac{1}{2J+1}\chi\sum_{\lambda=2,4}\Omega_\lambda\left\langle {}^5D_0\|U^{(\lambda)}\|{}^7F_J\right\rangle^2 \quad (2)$$

where $\chi = \frac{n_0(n_0^2+2)^2}{9}$ is the Lorentz local field correction and n_0 is the refractive index of the medium ($n_0 = 1.5$). The squared reduced matrix elements $\left\langle {}^5D_0\|U^{(\lambda)}\|{}^7F_J\right\rangle^2$ are tabulated in the literature [42], and their values are 0.0032 and 0.0023 for $J = 2$ and 4, respectively. The coefficients of spontaneous emission ($A_{0\rightarrow J}$), are obtained from:

$$A_{0\rightarrow J} = \left(\frac{\sigma_{0\rightarrow 1}}{S_{0\rightarrow 1}}\right)\left(\frac{S_{0\rightarrow J}}{\sigma_{0\rightarrow J}}\right)A_{0\rightarrow 1} \quad (3)$$

where $S_{0\rightarrow J}$ corresponds to the area under the curve related to the transition $^5D_0 \rightarrow {}^7F_J$ and $\sigma_{0\rightarrow J}$ is the energy barycenter of the transition.

The emission quantum efficiency (η) of the $^5D_0$ excited state is determined according to the following expression [43]:

$$\eta = \frac{A_{rad}}{A_{rad} + A_{nrad}}. \quad (4)$$

Table 1
Experimental intensity parameters (Ω_λ) (10^{-20} cm^{-2}), lifetimes τ (ms), emission coefficient rates A_{rad} (s^{-1}) A_{nrad} (s^{-1}), and emission quantum efficiencies η (%) for Eu-TTA complex and Eu-TTA-Si material.

Samples	Ω_2 (10^{-20} cm^{-2})	Ω_4 (10^{-20} cm^{-2})	A_{rad} (s^{-1})	A_{nrad} (s^{-1})	A_{tot} (s^{-1})	τ (ms)	η (%)
Eu-TTA	32	5	1168	3180	4348	0.23	27
Eu-TTA-Si	8	9	410	2090	2500	0.40*	16

* $\tau_{average} = (A_1\tau_1^2) + (A_2\tau_2^2)/(A_1\tau_1 + A_2\tau_2)$, where τ_1 and τ_2 are short- and long-lifetimes, with corresponding intensity coefficients A_1 and A_2.

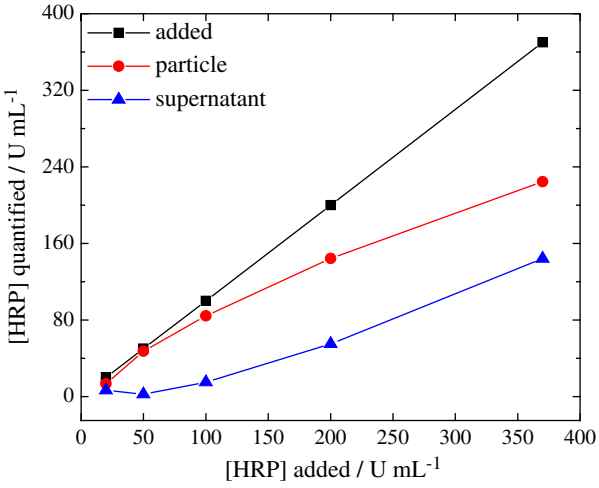

Fig. 9. Quantification of the HRP units in the Eu-TTA-Si-GA-Ag-Ab-GA-HRP system as a function of the enzyme content added.

The total decay rate corresponds to $A_{tot} = \frac{1}{\tau} = A_{rad} + A_{nrad}$, where $A_{rad} = \sum_J A_{0\rightarrow J}$ and A_{nrad} are the total radiative and non-radiative rates, respectively.

A decrease is observed in the value of the parameter Ω_2 of the Eu-TTA-Si material when compared with the complex, due to the reduced intensity of the $^5D_0 \rightarrow {}^7F_2$ transition. This fact together with the higher value of the intensity parameter Ω_4 for the system with silica, Eu-TTA-Si, reflects the highly uncommon intensity of the $^5D_0 \rightarrow {}^7F_4$ transition observed in the emission spectra, corroborating with the proposal discussed in Refs. [44,45] in which these two facts indicate that the site symmetry of the rare earth ion has changed towards higher symmetry. The value of the quantum efficiency (η) of the Eu-TTA-Si material (Table 1) is lower than the one determined for the precursor complex. This result is a consequence of the considerably more accentuated decrease of the radiative contribution (A_{rad}) to the total decay rate, in spite of the decrease in the nonradiative component (A_{nrad}).

3.2. Antigen-antibody reaction

In order to verify the occurrence of the Ag–Ab reaction on the surface of the Eu-TTA-Si particle, the assay was performed using the Ag coupled with the HRP enzyme. The system used was the Eu-TTA-Si particle-GA-anti-oxLDL antibody that reacts with HRP-GA-oxLDL. Then, the concentration of the HRP was determined by colorimetric assay using an enzyme-substrate reaction. The formed Schiff bases from the reaction of the amino and aldehyde groups were reduced with the addition of sodium borohydride. However, the remaining aldehyde groups of the spacer GA were blocked by adding glycine.

The absorbance data were recorded using an ELISA plate reader, whereas the degree of color development in each well is proportional to the concentration of the enzyme. Fig. 9 illustrates the HRP concentration calculated in the Eu-TTA-Si particle-GA-anti-oxLDL antibody-oxLDL-GA-HRP system which varies in the oxLDL-GA-HRP conjugate. These data were obtained by the difference between the initial amount of added HRP and the one measured in the supernatant, resulting in a quantification of the HRP in the Eu-TTA-Si particle-GA-anti-oxLDL antibody-oxLDL-GA-HRP system.

The absorbance results showed that with increasing concentration of the HRP, 20 to 370 U mL^{-1}, an increase in the enzyme–substrate reaction is observed. Moreover, with the maximum concentration of the enzyme used (370 U mL^{-1}) they did not observe the occurrence of saturation of the system. It was also noted the absence of enzyme in the washings, indicating that the Ag–Ab linkage is stable.

4. Conclusion

The Eu-TTA-Si luminescent marker was effectively prepared by the Stöber method. IR, SEM and XRD analyses suggest that the complex precursor interacts with the silica network. The ninhydrin method confirmed the presence of the amino groups in the particle surface and showed the capacity of these groups to react with the glutaraldehyde spacer. The assay using the enzyme HRP-tagged antigen demonstrated the ability of the aminated silica particles to interact with biomolecules. These data open new area for the development of protein-tagged luminescent particles for use in biomedical sciences. The particles and the conjugate that were developed in this study are potential candidates for development of the protocol for the quantification of the oxLDL or for the study of atherosclerotic process.

Acknowledgments

This work was supported by CAPES (Coordenação de Aperfeiçoamento de Pessoal de Nível Superior), CNPq (Conselho Nacional de Desenvolvimento Científico e Tecnológico) and FAPESP (Fundação de Amparo à Pesquisa do Estado de São Paulo) Brazilian agencies, Nanobiotec-Brazil/CAPES (Coordenação de Aperfeiçoamento de Pessoal de Nível Superior) and INCT-INAMI (Instituto Brasileiro de Nanotecnologia para Marcadores Integrados — CNPq).

References

[1] A.G. Macedo, M.A. Martins, S.E.M. Fernandes, A. Barros-Timmons, T. Trindade, L.D. Carlos, J. Rocha, Opt. Mater. 32 (2010) 1622–1628.
[2] A.V.S. Lourenço, C.A. Kodaira, E.R. Souza, M.C.F.C. Felinto, O.L. Malta, H.F. Brito, Opt. Mater. 33 (2011) 1548–1552.
[3] B. Cojocaru, C. Tiseanu, V.I. Parvulescu, J. Non-Cryst. Solids 356 (2010) 1854–1858.
[4] K. Binnemans, Chem. Rev. 109 (2009) 4283–4374.
[5] A.P. Duarte, M. Gressier, M.-J. Menu, J. Dexpert-Ghys, J.M.A. Caiut, S.J.L. Ribeiro, J. Phys. Chem. C 116 (2012) 505–515.
[6] L. Tian, Z. Dai, L. Zhang, R. Zhang, Z. Ye, J. Wu, D. Jin, J. Yuan, Nanoscale 4 (2012) 3551–3557.
[7] Y. Wu, X. Xu, Q. Tang, Y. Li, Nanotechnology 23 (2012) 205103.
[8] S.L.C. Pinho, H. Faneca, C.F.G.C. Geraldes, M.-H. Delville, L.D. Carlos, J. Rocha, Biomaterials 33 (2012) 925–935.
[9] Y. Zhou, X. Xia, Y. Xu, W. Ke, W. Yang, Q. Li, Anal. Chim. Acta 722 (2012) 95–99.
[10] A.A.S. Araujo, H.F. Brito, O.L. Malta, J.R. Matos, E.E.S. Teotonio, S. Storpirtis, C.M.S. Izumi, J. Inorg. Biochem. 88 (2002) 87–93.
[11] C.A. Kodaira, A.V.S. Lourenço, M.C.F.C. Felinto, E.M.R. Sanchez, F.J.O. Rios, L.A.O. Nunes, M. Gidlund, O.L. Malta, H.F. Brito, J. Lumin. 131 (2011) 727–731.
[12] H.F. Brito, O.L. Malta, H.F. Brito, O.L. Malta, M.C.F.C. Felinto, E.E.S. Teotonio, The Chemistry of Metal Enolates, in: J. Zabicky (Ed.), John Wiley & Sons Ltd., England, 2009, pp. 131–184.
[13] J. Kim, J.E. Lee, J. Lee, J.H. Yu, B.C. Kim, K. An, Y. Hwang, C.H. Shin, J.G. Park, J. Kim, T.J. Hyeon, J. Am. Chem. Soc. 128 (2006) 688–689.
[14] D.K. Yi, S.T. Selvan, S.S. Lee, G.C. Papaefthymiou, D. Kundaliya, J.Y. Ying, J. Am. Chem. Soc. 127 (2005) 4990–4991.
[15] D. Kehrloesser, R.-P. Baumann, H.-C. Kim, N. Hampp, Langmuir 27 (2011) 4149–4155.
[16] R. Stocker, J.F. Keaney Jr., Physiol. Rev. 84 (2004) 1381–1478.
[17] R. Ross, Nature 362 (1993) 801–809.
[18] J.L. Fernandes, J.L. Orford, C. Garcia, O.R. Coelho, M. Gidlund, M.H.S.L. Blotta, J. Autoimmun. 23 (2004) 345–352.
[19] M. Gidlund, N.R.T. Damasceno, D.S.P. Abdalla, H. Goto, Braz. J. Med. Biochem. Res. 29 (1996) 1625–1628.
[20] L. Van Tits, J. De Graaf, H. Hak-Lemmers, S. Bredie, P. Demarker, P. Holvoet, A. Stalenhoef, Lab. Invest. 83 (2003) 13–21.
[21] W. Stöber, A. Fink, E. Bohn, J. Colloid Interface Sci. 26 (1968) 62–69.
[22] O.L. Malta, H.F. Brito, J.F.S. Menezes, F.R. Gonçalves e Silva, S. Alves Jr., F.S. Farias Jr., A.V.M. de Andrade, J. Lumin. 75 (1997) 255–268.
[23] J. Kai, D.F. Parra, H.F. Brito, J. Mater. Chem. 18 (2008) 4549–4554.
[24] J. Zhang, Y. Fu, J.R. Lakowicz, J. Phys. Chem. C 111 (2007) 1955–1961.
[25] N.R.T. Damasceno, H. Goto, F.M.D. Rodrigues, C.T.S. Dias, F.S. Okawabata, D.S.P. Abdalla, M. Gdilund, J. Nutr. 130 (2000) 2641–2647.
[26] D.F. Ketelhuth, G.C. Tonini, M.D.T. Carvalho, R.F. Ramos, P. Boschcov, M. Gidlund, Scand. J. Immunol. 68 (2008) 456–462.
[27] E.C. Fernvik, D.F.J. Ketelhuth, M. Russo, M. Gidlund, J. Clin. Immunol. 24 (2004) 170–176.
[28] J.L. Liu, B. Yan, J. Phys. Chem. B 112 (2008) 10898–10907.
[29] C. Ren, J. Li, J. Sun, X. Chen, Z. Hua, D. Xue, J. Lumin. 130 (2010) 65–69.
[30] H. Hoffmann, P.B. Staudt, T.M.H. Costa, C.C. Moroand, E.V. Benvenutti, Surf. Interface Anal. 33 (2002) 631–634.

[31] B. Feng, R.Y. Hong, L.S. Wang, L. Guo, H.Z. Li, J. Ding, Y. Zheng, D.G. Wei, Colloids Surf. A 328 (2008) 52–59.
[32] P. Yang, Z. Quan, L. Lu, S. Huang, J. Lin, Biomaterials 29 (2008) 692–702.
[33] M. Yu, J. Lin, J. Fang, Chem. Mater. 17 (2005) 1783–1791.
[34] D. Shapilov, V.G. Kayumov, A.I. Krashenyuk, J. Anal. Chem. USSR 38 (1983) 436–438.
[35] I. Taylor, A.G. Howard, Anal. Chim. Acta 271 (1993) 77–82.
[36] P.A. Santa-Cruz, F.S. Teles, SpectraLux Software v.1.0, Ponto Quântico Nanodispositivos/RENAMI, 2003.
[37] V. Divya, S. Biju, R.L. Varma, M.L.P. Reddy, J. Mater. Chem. 20 (2010) 5220–5227.
[38] X. Guo, L. Fu, H. Zhang, L.D. Carlos, C. Peng, J. Guo, J. Yu, R. Denga, L. Sun, New J. Chem. 29 (2005) 1351–1358.
[39] G.S. Ofelt, J. Chem. Phys. 37 (1962) 511–520;
B.R. Judd, Phys. Rev. 127 (1962) 750–761.
[40] W.M. Faustino, S.A. Junior, L.C. Thompson, G.F. de Sá, O.L. Malta, A.M. Simas, Int. J. Quantum Chem. 103 (2005) 572–579.
[41] O.L. Malta, M.A.C. dos Santos, L.C. Thompson, N.K. Ito, J. Lumin. 69 (1996) 77–84.
[42] W.T. Carnall, H. Crosswhite, H.M. Crosswhite, Energy structure and transition probabilities of the trivalent lanthanides in LaF_3, Argonne National Laboratory Report, 1977, (unnumbered).
[43] G.F. Sá, O.L. Malta, C.D. Donega, A.M. Simas, R.L. Longo, P.A. Santa-Cruz, E.F. Silva Jr., Coord. Chem. Rev. 196 (2000) 165–195.
[44] R.A.S. Ferreira, S.S. Nobre, C.M. Granadeiro, H.I.S. Nogueira, L.D. Carlos, O.L. Malta, J. Lumin. 121 (2006) 561–567.
[45] M. Bettinelli, A. Speghini, F. Piccinelli, A.N.C. Neto, O.L. Malta, J. Lumin. 131 (2011) 1026–1028.